SAND98-2259J

Theoretical limit to the laser threshold current density in an InGaN quantum well laser

W.W.Chow,[a] H. Amano[b] and J. Han

Sandia National Laboratories

Albuquerque, NM 87185-0601, U. S. A.

T. Takeuchi

Department of Electrical and Electronic Engineering

Meijo University

1-501 Shiogamaguchi

Tempaku-ku, Nagoya 468, Japan

(September 17, 1998)

Abstract

This paper describes an investigation of the spontaneous emission limit to the laser threshold current density in an InGaN quantum well laser. The peak gain and spontaneous emission rate as functions of carrier density are computed using a microscopic laser theory. From these quantities, the minimum achievable threshold current density is determined for a given threshold gain. The dependence on quantum well width, and the effects of inhomogeneous broadening due to spatial alloy variations are discussed. Also, comparison with experiments is made.

a) Electronic mail: wwchow@somnet.sandia.gov

b) Permanent address: Department of Electrical and Electronic Engineering, Meijo University, 1-501 Shiogamaguchi, Tempaku-ku, Nagoya 468, Japan

DISCLAIMER

This report was prepared as an account of work sponsored by an agency of the United States Government. Neither the United States Government nor any agency thereof, nor any of their employees, makes any warranty, express or implied, or assumes any legal liability or responsibility for the accuracy, completeness, or usefulness of any information, apparatus, product, or process disclosed, or represents that its use would not infringe privately owned rights. Reference herein to any specific commercial product, process, or service by trade name, trademark, manufacturer, or otherwise does not necessarily constitute or imply its endorsement, recommendation, or favoring by the United States Government or any agency thereof. The views and opinions of authors expressed herein do not necessarily state or reflect those of the United States Government or any agency thereof.

DISCLAIMER

Portions of this document may be illegible in electronic image products. Images are produced from the best available original document.

Group-III nitride lasers are important because of the many optoelectronic technologies that require coherent emission in the blue-green wavelength region. [1] As these lasers are in an early developmental stage, there is interest in developing an understanding of physical mechanisms, expected device performance, and optimal laser configurations. At present, these issues are difficult to address experimentally because of the difficulty in growing high quality structures of known compositions. This paper approaches the problem from a theoretical aspect, focusing in particular on the estimation of laser threshold behaviors.

A number of groups have analyzed nitride based lasers. Owing to the strong Coulomb interactions in wide bandgap compounds, such as the group-III nitrides, a many-body gain model is required. Earlier investigations [2,3,5,4] used a gain model based on the Padé approximation to the semiconductor Bloch equations [6]. They demonstrated that the many-body effects, which are treated in the screened Hartree-Fock limit, significantly enhanced the gain. There are also distinct characteristics, such as a large (>100 meV) red shift of the emission wavelength with respect to the unexcited bandgap [2–4], as observed in experiments. [7] However, the model has some shortcomings. An important one is the use of the relaxation rate approximation to describe collision effects. With this approximation, the predictions of important quantities, such as peak gain and transparency carrier density, are sensitive to the dephasing rate, which is an input parameter that is usually determined from experiments. Because of insufficient experimental data, there is no reliable estimation of this parameter for nitride structures. It has also been shown that the relaxation rate approximation leads to inaccurate predictions of certain features of the semiconductor gain spectrum. [8]

To circumvent the relaxation rate approximation, the derivation of the semiconductor Bloch equations was extended beyond the Hartree-Fock contributions, to include higher order correlations describing carrier-carrier collisions. This approach eliminates the dephasing rate as a free parameter. Equally important, the more accurate description of collision effects results in good agreement with experimental gain and absorption spectra for wide ranges of carrier densities and laser materials. [8,9] The approach was applied to group-III

nitride quantum well lasers, resulting in a consistent treatment of optical behaviors from low electron and hole densities, where excitons are important, to high carrier densities, where an interacting Coulomb correlated electron-hole plasma determines the gain medium properties. [10] Gain spectra were computed, from which the dependences of the peak gain and gain peak energy on carrier density were studied. The effects of inhomogeneous broadening due to quantum well composition and width variations were also examined. However, the question of lasing threshold current density was not addressed, as it requires the conversion from carrier density to current density.

This paper furthers the investigation to include the calculation of spontaneous emission spectra, where predictions of threshold current densities may be made. We first review the gain spectrum calculation for a group-III nitride quantum well structure at different carrier densities. Using a relationship based on energy balance, [11] the spontaneous emission spectra are calculated from the gain spectra. From these two sets of spectra, we obtain a plot of the threshold gain, which depends on the optical resonator geometry and losses, versus the spontaneous emission current, which is the theoretical limit to the threshold current density. We show examples of plots for different quantum well structures and compare them to experiments. The effects of inhomogeneous broadening due to composition variations in the quantum well are discussed.

The calculation of gain involves the numerical solution of the equation of motion for the microscopic polarization, [10]

$$\frac{d}{dt}p_{\vec{k}}^{\nu_e,\nu_h} = -i\omega_{\vec{k}}^{\nu_e,\nu_h}p_{\vec{k}}^{\nu_e,\nu_h} - i\Omega_{\vec{k}}^{\nu_e,\nu_h}\left(n_{\vec{k}}^{\nu_e} + n_{\vec{k}}^{\nu_h} - 1\right) - \left(\Gamma_{\vec{k}}^{\nu_e} + \Gamma_{\vec{k}}^{\nu_h}\right)p_{\vec{k}}^{\nu_e,\nu_h} + \sum_{\vec{q}}\left(\Gamma_{\vec{k},\vec{q}}^{\nu_e} + \Gamma_{\vec{k},\vec{q}}^{\nu_h}\right)p_{\vec{k}+\vec{q}}^{\nu_e,\nu_h} \quad . \tag{1}$$

where $\nu_e(\nu_h)$ identifies the conduction (valence) quantum well subband and $n_{\vec{k}}^{\nu_e}(n_{\vec{k}}^{\nu_h})$ are the carrier distributions. The first two terms on the right hand side describe the oscillation of the polarization at the transition frequency, $\omega_{\vec{k}}^{\nu_e,\nu_h}$, and the stimulated emission and absorption processes. The many-body effects appear as a carrier density (N) dependence in the transition energy, the Rabi frequency $\Omega_{\vec{k}}^{\nu_e,\nu_h}$. Carrier-carrier correlations, which lead

to screening and dephasing, give rise to the last two terms in Eq. (1). These contributions are treated at the level of quantum kinetic theory in the Markovian limit. They consist of diagonal ($p_{\vec{k}}^{\nu_e,\nu_h}$ term) and nondiagonal ($p_{\vec{k}+\vec{q}}^{\nu_e,\nu_h}$ term) contributions. The former describes dephasing, while the latter, which is important in achieving agreement with experiments, is neglected in relaxation rate treatments. We limit our discussion to the small signal gain, where the carrier populations $n_{\vec{k}}^{\nu}$ are inputs to the calculations. The steady state solution to the polarization equation at an input laser field and carrier density is used in the following semiclassical expression for the intensity gain G (MKS units): [6]

$$G = -\frac{2\omega}{\varepsilon_0 ncV\mathcal{E}} \mathrm{Im}\left(\sum_{\nu_e,\nu_h,\vec{k}} \left(\mu_{\vec{k}}^{\nu_e,\nu_h}\right)^* p_{\vec{k}}^{\nu_e,\nu_h} e^{i\omega t} \right) \quad , \tag{2}$$

where $\mathcal{E}$ is the slowly varying electric field amplitude, ω is the laser frequency, ε_0 and c are the permittivity and speed of light in vacuum, n is the background refractive index, and V is the active region volume.

The bandstructure properties, specifically the electron and hole energy dispersions, $\varepsilon_{\vec{k}}^{\nu_e}$ and $\varepsilon_{\vec{k}}^{\nu_h}$, respectively, and the optical dipole matrix element $\mu_{\vec{k}}^{\nu_e,\nu_h}$, are inputs to the gain calculation. These quantities, for InGaN and GaN grown pseudomorphically along the c axis of the hexagonal wurzite crystal structure, are computed using a 6×6 Luttinger-Kohn Hamiltonian and the envelope approximation [12]. Input parameters are the bulk wurtzite material parameters. For the calculations described in this paper, we use the values listed in Ref. (13).

We begin by calculating the room temperature gain spectra for a range of carrier densities. From these spectra, we extract the peak gain as a function of carrier density. Figure 1(top) shows the curves for the $2nm$ and $4nm$ $In_{0.2}Ga_{0.8}N$-GaN quantum well structures, which are representative of the laser gain regions presently used in experiments. Only the TE (polarization in the plane of the quantum well) curves are plotted, because the TM gain is negligible for experimentally realizable carrier densities. The figure shows that significantly higher carrier densities are required to achieve gain in the $4nm$ structure. This is because the piezoelectric field, [14] due to the strain in the quantum well, causes an appre-

ciable separation between the electron and hole eigenfunctions in the wide $4nm$ quantum well. This spatial separation reduces the optical dipole matrix element. As a result, a high carrier density is necessary to screen the piezoelectric field and restore the dipole matrix element. In the case of the $2nm$ quantum well, the relative displacement of the electron and hole eigenfunctions is limited by the narrow quantum well width, so that the dipole matrix element is not as significantly reduced. A sharp increase in the influence of the piezoelectric field on the dipole matrix element occurs at well widths around 3 to $3.5nm$ in the $In_{0.2}Ga_{0.8}N$-GaN structure, when the bandstructure changes from having one confined electron subband to two confined electron subbands.

To convert from carrier density to current density, we compute the spontaneous emission spectrum by using the phenomenological relationship [11],

$$se(\omega) = \frac{1}{\hbar}\left(\frac{n\omega}{\pi c}\right)^2 g(\omega)\left[\exp\left(\frac{\hbar\omega - \mu_{eh}}{k_B T}\right) - 1\right]^{-1} \quad , \tag{3}$$

where k_B is the Boltzmann constant, and μ_{eh} is electron-hole quasi-chemical potential energy separation. Integrating the spectrum gives the spontaneous emission rate,

$$w_{sp} = \int_0^\infty d\omega \; se(\omega) \; . \tag{4}$$

Figure 1(bottom) shows w_{sp} as a function of carrier density for the $2nm$ and $4nm$ $In_{0.2}Ga_{0.8}N$-GaN quantum well structures. The figure shows that there is already significant spontaneous emission at transparency for the $2nm$ quantum well. On the other hand, because of the reduction in the dipole matrix element by the piezoelectric field, the $4nm$ quantum well is able to sustain a large population inversion without high spontaneous emission loss.

We obtain Fig. 2 by using Fig. 1 and $J_{sp} = ewv_{sp}$ for the spontaneous emission contribution to the injection current density, where e is the electron charge, and w is the quantum well width. The solid curves show the threshold gain versus spontaneous emission current density for the homogeneously broadened samples, with no alloy or dimensional fluctuations. For minimum threshold current density, we assume operation at the gain peak, and neglect contributions from nonradiative and carrier transport losses. An interesting

result is the prediction of lower threshold current density for the $4nm$ quantum well, because of lower spontaneous emission loss. However, we emphasize that because of the high carrier densities necessary for gain, the $4nm$ structure is more susceptible to nonradiative carrier losses. The dashed and dotted curves show the effects of inhomogeneous broadening due to In concentration variations in the quantum well, of standard deviations $\sigma_{In} = 0.2$ and 0.4, respectively. The two structures show noticeable difference in their dependences on alloy fluctuations. This difference comes from the $4nm$ quantum well having significantly broader gain bandwidths than the $2nm$ structure, because it operates at higher carier densities.

Figure 2 also shows experimental data obtained from devices listed in Table I. The material threshold gain is computed using

$$G_{th} = \frac{1}{\Gamma}\left[\alpha_i - \frac{1}{L}\ln\left(R_1 R_2\right)\right] , \tag{5}$$

where we obtain from the references the values for the facet reflectivity and resonator length, $R_{1(2)}$ and L, respectively. We assume $\alpha_i = 40cm^{-1}$ for the internal optical losses, and compute the confinement factor Γ from information provided on the quantum well, barrier and cladding layers dimensions and compositions. Furthermore, we assume that the material threshold current $J_{th} = J_{\exp}/N$, where N is the number of quantum wells and $J_{\exp}$ is the measured threshold current density. The experimental data are grouped into two categories: those with quantum well width $w < 3.5nm$ and those with $w \geq 3.5nm$. As discussed earlier, the former should have dipole matrix elements not appreciably reduced by the piezoelectric field. On the hand, the latter should have significantly smaller dipole matrix elements at low carrier densities where the piezoelectric field is largely unscreened. Figure 2 shows surprising closeness of some of the experimental threshold current densities to the spontaneous emission limit predicted for the homogeneously broadened structures. With the exception of one data point (Nichia1), all the experimental data lie to higher current density side of the theoretical limit (solid curves). The one discrepancy may be due to differences in calculated and experimental configurations (e.g. well widths of $2nm$ versus $2.5nm$, respectively), sensitivity of the numerical calculations to step sizes at low gain, inacurracies in Eq. (3)

close to transparency, and uncertainty in the experimental threshold current density.

In summary, this paper investigates the theoretical limit to the threshold current density in InGaN quantum well lasers. The analysis is based on a microscopic theory where carrier-carrier collisions are treated at the level of quantum kinetic theory. This leads to an improvement in predictive capability over the conventional relaxation rate gain models, because the dephasing rate is not a free parameter. The investigation shows a dependence of the theoretical limit on the quantum well width, due partly to the spatial displacement of the carriers by the piezoelectric effect. Comparison between theory and experiment suggests that some of the experimental devices are operating close to the spontaneous emission limit for the particular laser configuration.

This work was supported in part by the U. S. Department of Energy under contract No. DE-AC04-94AL85000.

Sandia is a multiprogram laboratory operated by Sandia Corporation, a Lockheed Martin Company, for the United States Department of Energy under contract DE-AC04-94AL85000.

References

[1] S. Nakamura and G. Fasol, *The Blue Laser Diode* (Springer, Berlin, 1997).

[2] W. W. Chow, A. Knorr and S. W. Koch, Appl. Phys. Lett. **67**, 754 (1995).

[3] W. W. Chow, A. F. Wright and J. S. Nelson, Appl. Phys. Lett. **68**, 296 (1996).

[4] S.-H. Park and D. Ahn, Appl. Phys. Lett., **71**, 398 (1997).

[5] S. H. Park and S. L. Chuang, APL **72** 287 (1998).

[6] W. W. Chow, S. W. Koch and M. Sargent III, *Semiconductor-Laser Physics* (Springer, Berlin, 1994).

[7] H. Sakai, T. Takeuchi, H. Amano and I. Akasaki, The Review of Laser Engineering **25**, 510 (1997).

[8] W. W. Chow, P. M. Smowton, P. Blood, A. Girndt, F. Jaknke and S. W. Koch, Appl. Phys. Lett. **71**, 157 (1995).

[9] A. Girndt, S. W. Koch and W. W. Chow, Appl. Phys. A **66**, 1 (1998).

[10] W. W. Chow, A.F. Wright, A. Girndt, F. Jahnke and S. W. Koch, Appl. Phys. Lett. **71**, 2608 (1997).

[11] C. H. Henry, R. A. Logan and F. R. Merritt, J. Appl. Phys. **51**, 3042 (1980).

[12] S. L. Chuang and C. S. Chang, Phys. Rev. B **54** 2491 (1996).

[13] W. W. Chow, M. H. Crawford, A. Girndt and S. W. Koch, IEEE J. Selected Topics in Quantum Electron. **4**, 514 (1998).

[14] A. Bykhovshi, B. Gelmonst and M. Shur, J. Appl. Phys. **74**, 6734 (1993).

[15] K. Itaya, M. Onomura, J. Nishio, L. Sugiura, S. Saito, M. Suzuki, J. Rennie, S. Nunoue, M. Yamamoto, H. Fujimoto, H. Kokubun, Y. Ohba, G. Hatakoshi and M. Ishikawa, Jpn. J. Appl. Phys. **35**, L1315 (1996).

[16] M. P. Mack, A. Abare, M. Aizcorbe, P. Kozodoy , S. Keller, U. K. Mishra, L. Coldren and S. P. DenBaars, MIJ-NSR **2**, Art. 41 (1997).

[17] M. Kneissel, D. P. Bour, N. M. Johnson, L. T. Lomano, B. S. Krusor, R. Donaldson, J. Walker and C. Dunnrowicz, Appl. Phys. Lett. **72**,1539 (1998).

[18] N. Yamada, Y. Kaneko, S. Watanabe, Y. Yamaoka, T. Hidaka, S. Nakagawa, E. Marenger, T. Takeuchi, S. Yamaguchi, H. Amano and I. Akasaki, 10th IEEE/Lasers and Electro-Optics Society Annual Meeting, PD1.2 (1997).

[19] F. Nakamura, T. Kobayashi, T. Tojo, T. Asatsuma, K. M. Naganuma, H. Kawai and M. Ikeda, Electron. Lett. **34**, 1105 (1998).

[20] S. Nakamura, M. Senoh, S. Nagahama, N. Iwasa, T. Yamada, T. Matsuoka, H.Kiyoku, Y. Sugimoto, Jpn. J. Appl. Phys. **35**, L74 (1996).

[21] S. Nakamura, M. Senoh, S. Nagahama, N. Iwasa, T. Yamada, T. Matsuoka, H.Kiyoku, Y. Sugimoto, T. Kozaki, H. Umemoto, M. Sano, Y. Chocho, Jpn. J. Appl. Phys. **36**, L1568 (1997).

[22] S. Nakamura, M. Senoh, S. Nagahama, N. Iwasa, T. Yamada, T. Matsuoka, H.Kiyoku, Y. Sugimoto, T. Kozaki, H. Umemoto, M. Sano, Y. Chocho, Appl. Phys. Lett. **72**, 211 (1998).

Figure Captions

Figure 1. Calculated (top) TE peak gain and (bottom) spontaneous emission rate vs. carrier density for $2nm$ and $4nm$ $In_{0.2}Ga_{0.8}N/GaN$ quantum well at $T = 300K$.

Figure 2. Calculated TE threshold gain vs. spontaneous emission current for $2nm$ and $4nm$ $In_{0.2}Ga_{0.8}N/GaN$ quantum well at $T = 300K$. The curves are for homogeneous broadening (solid), $\sigma_{In} = 0.02$ (dashed) and 0.04 (dotted). The points are experimental results for quantum well width $w < 3.5nm$ (circles) and $w \geq 3.5nm$ (squares).

Table I. Experimental threshold gains and current densities.

Source	QW	Γ	$G_{th}(10^3/cm)$	$J_{th}(kA/cm^2/QW)$
Toshiba [15]	2nm $In_{0.15}Ga_{0.85}N$	0.20	0.222	2.00
UCSB [16]	3nm $In_{0.18}Ga_{0.82}N$	0.14	0.319	1.26
Xerox [17]	2nm $In_{0.20}Ga_{0.80}N$	0.07	0.622	2.40
Meijo/HP [18]	2nm $In_{0.10}Ga_{0.90}N$	0.06	0.786	3.00
Sony [19]	3nm $In_{0.11}Ga_{0.89}N$	0.05	0.902	1.90
Nichia1 [20]	2.5nm $In_{0.20}Ga_{0.80}N$	0.19	0.221	0.48
Nichia2 [21]	3.5nm $In_{0.15}Ga_{0.85}N$	0.04	1.067	0.75
Nichia3 [22]	3.5nm $In_{0.15}Ga_{0.85}N$	0.03	1.410	1.00

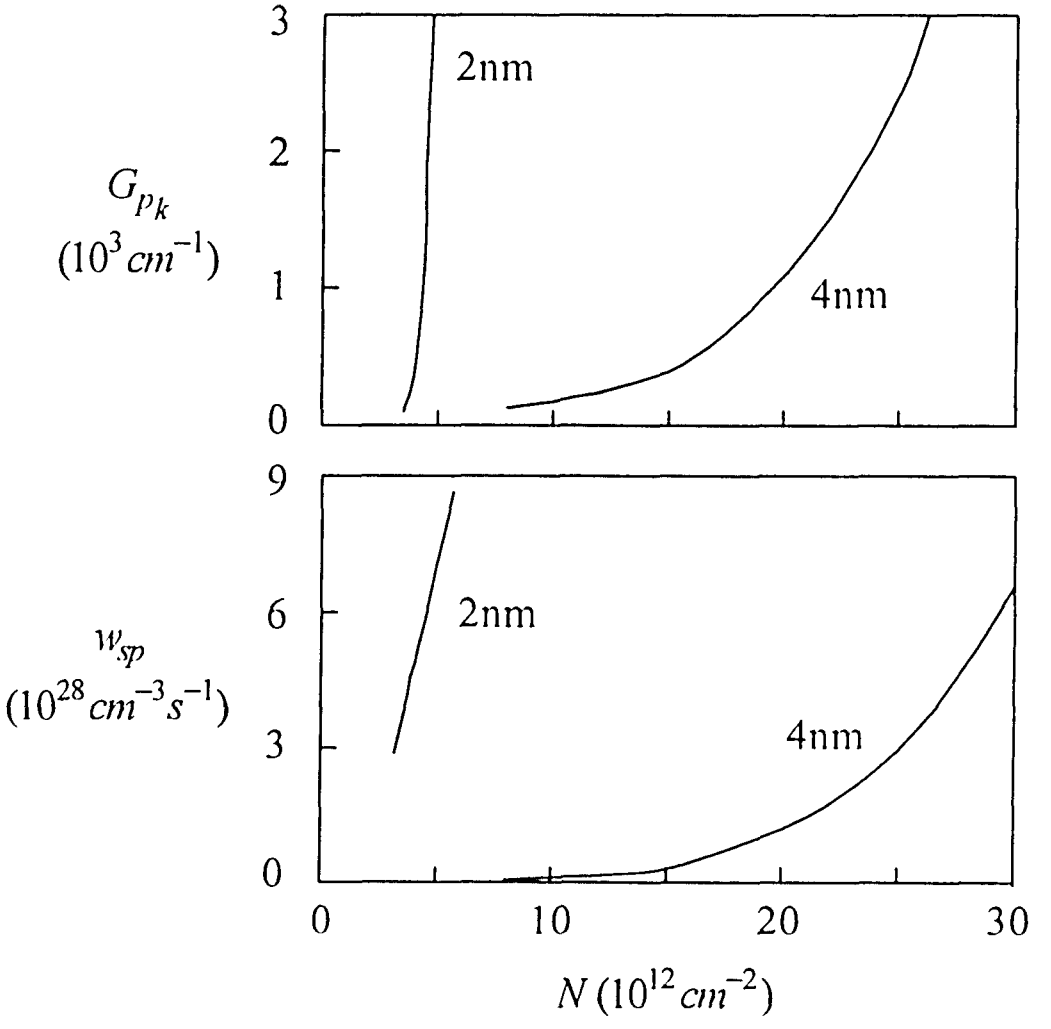

Fig. 1, APL, Chow

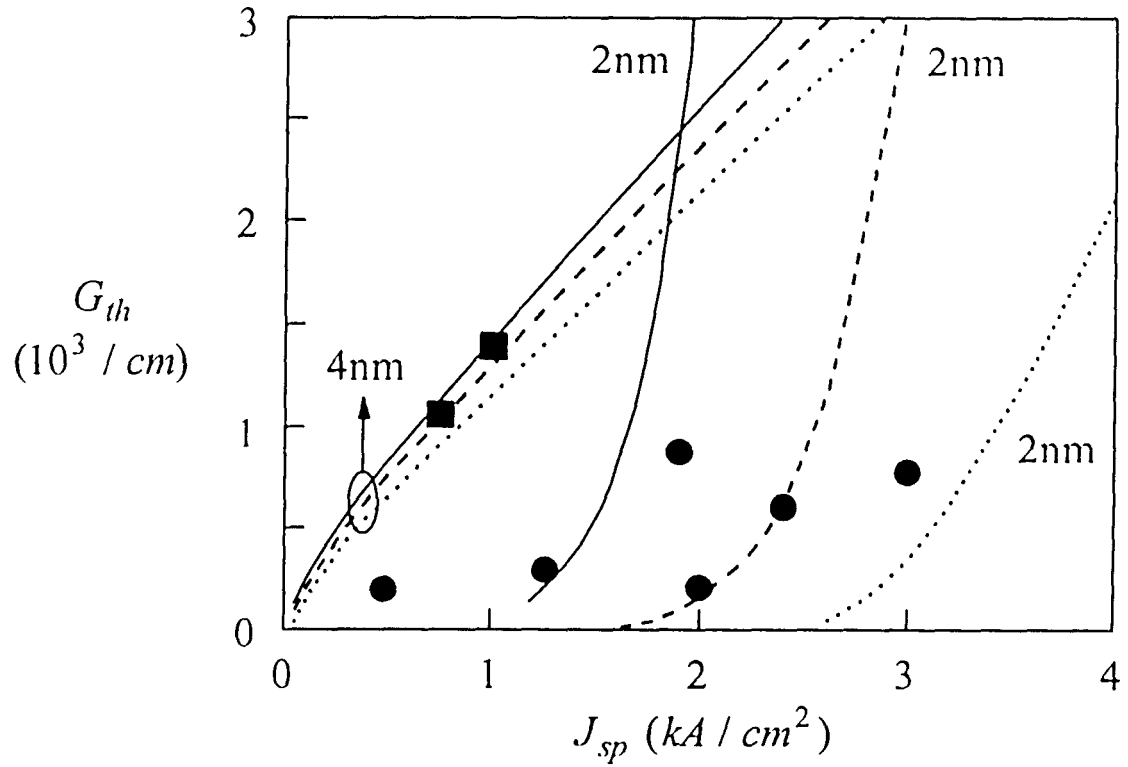

Fig. 2, APL, Chow